Figure 200: 12 km S. Akseki, Antalya, Turkey. Collection locality of *Iurus kadleci*, **sp. nov.**, and *I. kraepelini*, together with *Calchas gruberi* and *Mesobuthus gibbosus*.

The genital operculum of the male is dramatically different from that in the female (Figs. 189–190). The sclerites, subtriangular in shape, are as long as or longer than wide in the male, whereas in the female the sclerites are short and wide, more than twice as wide as long. Whereas the sclerites are fused medially in the female, they are separated along their entire length in the male, exposing significantly developed genital papillae. The enlarged genital operculum of the male extends distally between the lateral lobes of the sternum partially obscuring its proximal region. Figures 196–200 show dorsal and ventral views of both male and female specimens, and collection localities for this species. A subadult female collected deep inside the Dim Cave (Fig. 198) also exhibited a slender metasoma, all segments longer than wide.

Discussion. The chela is quite unique in *I. kadleci*. It has an exaggerated proximal gap in both male and female adults. The size of this gap is only matched in its sympatric species *I. kraepelini*. However, unique in *I. kadleci* is the presence of this gap in the female, unprecedented in *Iurus* (i.e., in other *Iurus* species the gap, if present, is only well-developed in adult males). The gap size is further exaggerated due to the slenderness of the chela, in particular its somewhat narrow depth (see discussion below). We can hypothesize here, when contrasted to the highly vaulted, deep chelal palm of *I. kraepelini*, that the somewhat thin palm of *I. kadleci* might contribute to the enlarged proximal gap seen in the female.

I. kadleci is considerably thinner than the other species of *Iurus*. This is exhibited in the metasomal segments, the telson, and the chela. The slender metasoma is even evident in a subadult female from the Dim Cave, with all segments longer than wide. As shown in the histograms in Appendix C (Figs. C4–C5), morphometric ratios constructed from the five metasomal segments, the telson length as compared to its width, and the chelal length as compared to its depth, exhibit complete standard error separation from the other four species in both genders. Mean value differences (MVD) between *I. kadleci* and the other four species are shown in Table 8.

Accompanying the thin metasoma of *I. kadleci* is the relatively large number of serrated spines comprising the dorsal carinae of segments I–IV, the largest in the genus. Table 9 compares average spine numbers across

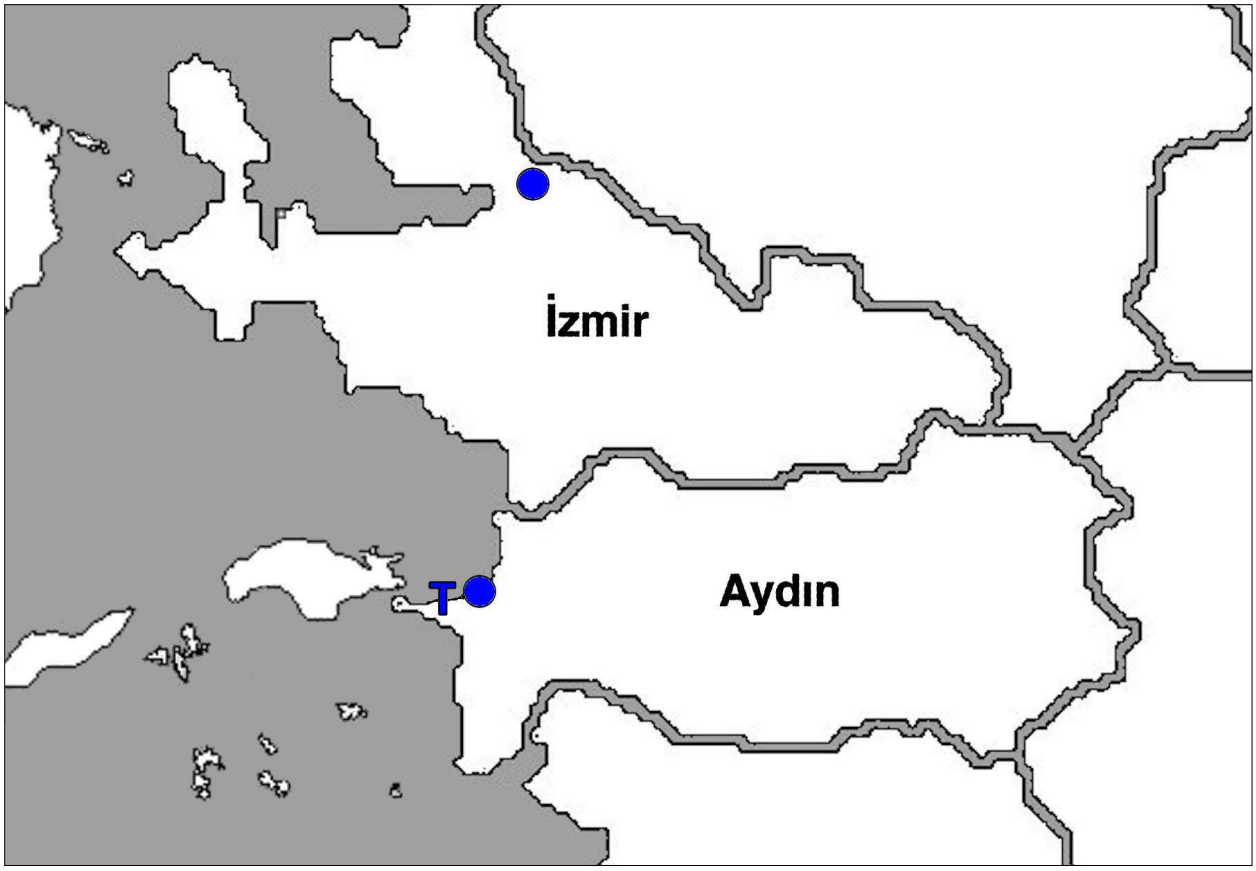

Figure 201: Large-scale map showing distribution of *Iurus kinzelbachi*, **sp. nov**. "T" marks type locality, Dilek Peninsula, Aydın Province, Turkey. See Fig. 74 for distribution of all species and Appendix A for detailed locality data.

the five species of *Iurus*. *I. dufoureius* has spine numbers approaching *I. kadleci* showing some standard error overlap, but still exhibiting a 16 percent mean value difference. The other species show no overlap with *I. kadleci*, including absolute ranges. *I. kraepelini* has the smallest number of spines on the dorsal carinae in the genus, with over a 55 % MVD from *I. kadleci*.

The mesosomal tergites of *I. kadleci* are essentially smooth on segments I–VI, the other *Iurus* species exhibit heavily granulose plates. The lateral carinae of metasomal segments I–IV are only developed on segment I in *I. kadleci*, whereas they occur on segments I–II to I–III in the other species.

Unfortunately, the hemispermatophore is unknown in *I. kadleci*. As seen in this paper, the hemispermatophore has proved to be an excellent diagnostic character, exhibiting major structural and morphometric differences across the four species where it has been examined. We suspect the hemispermatophore of *I. kadleci* when finally examined will be similar in structure to its sympatric species *I. kraepelini*, which is also its proposed sister taxon.

Thus far, not much is known about the habitat or microhabitat preferences of *I. kadleci*. In Akseki, two specimens were found in the same general habitat as *I. kraepelini*, and therefore are sympatric if not syntopic with the latter species. Presence of this species deep in Dim Cave, where it has been found hiding in a rock crevice (Fig. 198) might indicate its lithophilic and/or troglophilic nature. Its much lighter coloration than in all other *Iurus* species as well as its relative slenderness could indicate a specialized adaptation. We are currently attempting to locate more specimens with careful attention to their specific microhabitats. Detailed ecological information on Dim Cave and its fauna are presented in Kunt, Yağmur & Elverici (2008).

Material Examined (= type material, 5 specimens). Holotype: ♀ (FKCP), TURKEY, *Antalya Province*: Akseki District, 12 km S Akseki, 11–12 May 2006, leg. F. Kovařík. **Paratypes:** 1 ♀ (FKCP), 1 ♂ (VFWV), same label as holotype; Alanya District, Dim Cave, 11 km E of Alanya, 6°32'21"N, 32°06'33"E, cave entrance at 221 m asl, vertical depth 25 m, 22 April 2007, 1 ♂ sbad., leg. K. B. Kunt, G. Tunsley & R. Gabriel (MTAS). *Mersin Province*: Gülnar District, Gülnar, July 2000, 1 ♂, leg. R. Werner & R. Lízler (FKCP).

Iurus kinzelbachi Kovařík, Fet, Soleglad et Yağmur, sp. nov.

(Figs. 5, 13, 25, 37, 50–51, 60, 62–63, 73–74, 201–224; Tabs. 1–3, 10–11)

REFERENCES:

Iurus dufoureius: Kinzelbach, 1975: 25 (in part; "Marli Kioi"); Crucitti & Cicuzza, 2001: 227, 229, fig. 7 (in part; map plot near İzmir); Soleglad, Kovařík & Fet, 2009: 2–3 (in part; "Narli Kioi"), fig. 13–15 (in part).

Iurus dufoureius asiaticus: Koç & Yağmur, 2007: 57, fig. 4; Francke & Prendini, 2008: 218 (in part; Davutlar); Yağmur, Koç & Akkaya, 2009: 154–159 (in part: Aydın: Dilek).

Holotype: ♂ (NHMW), TURKEY, *Aydın Province*: Söke District, Dilek Peninsula National Park, Canyon, 37°41'37"N, 27°09'37"E, 82 m asl, 18 June 2005, leg. H. Koç. **Paratypes**, see list below.

Diagnosis. Medium sized species, 85 mm. Dark gray to black in overall coloration. Pectinal tooth counts lowest in genus, 10–12 (10.62) males, 8–11 (9.33) females. Chelal movable finger lobe in adults located on basal half, lobe ratio 0.38–0.47; proximal gap on fixed finger present in adult males; movable finger of adult males essentially straight, not highly curved; number of inner denticles (*ID*) of chelal movable finger, 13–15 (14); constellation array with *four* to *six* sensilla; hemispermatophore lamina internal nodule vestigial to obsolete, positioned very basally due to elongated lamina, lamina distal length / lamina basal length 4.313–5.107 (4.710), lamina terminus blunted, not pointed, terminus of acuminate process truncated, transverse trunk bolsters are present. Four unique types of neobothriotaxy found on external aspects of chela and patella, although not on all specimens or both pedipalps; at least one neobothriotaxic type has been detected on 80 % of specimens examined. Dominant morphometrics (see Appendix X) are chelal movable and fixed finger lengths.

Distribution. **Turkey** (west): İzmir (extinct?) and Aydın Provinces. See map in Fig. 201 for large-scale distribution of this species.

Etymology. We are honored to name this new species after our esteemed colleague Dr. Ragnar Kinzelbach (Rostock, Germany) who pioneered modern studies of scorpions from Greece and Turkey (Kinzelbach, 1975, 1982, 1985, etc).

MALE. The following description is based on holotype male from Dilek Peninsula National Park, Aydın, Turkey. Measurements of the holotype plus two other specimens are presented in Table 10. See Figure 202 for a dorsal and ventral view of the male holotype.

COLORATION. Basic color of carapace, mesosoma, metasoma, telson, and pedipalp blackish-brown; legs a lighter mahogany color, tarsus yellowish; cheliceral fingers and distal aspect of palm purplish, proximal aspect of palm yellowish; pedipalp and dorsal metasomal carinae blackish; sternites mahogany; genital operculum, basal piece and pectines yellow-tan. Eyes and tubercles black, leg condyles and aculeus tip dark brown. No patterns present.

CARAPACE (Fig. 203). Anterior edge with a conspicuous median indentation, approximately twelve irregularly placed setae visible; entire surface densely covered with small to medium granules. Mediolateral ocular carinae well-developed and granulated, extending to the lateral eyes; there are three lateral eyes, the posterior eye the smallest. Median eyes and tubercle of medium size, positioned anterior of middle with the following length and width formulas: 394|1040 and 143|917.

MESOSOMA (Figs. 206, 208). Tergites I–VII densely populated with minute granules; tergite VII lateral carinae serrated, median carinae obsolete, essentially obscured by coarse granulation. Sternites III–VI smooth and lustrous; VII with scattered lateral granulation, one pair of irregularly granulated lateral carinae and one pair of smooth median carinae (Fig. 208). Stigmata (Fig. 206) are medium in size and slit-like in shape, angled 45° in an anterointernal direction.

METASOMA (Fig. 205). Segment I wider than long. Segments I–IV: dorsal and dorsolateral carinae serrated; dorsal carinae with 10/12, 10/10, 9/10, and 10/9 serrated spines (left/right carina); dorsal (I–IV) and dorsolateral (I–III) carinae do not terminate with an enlarged spine; lateral carinae serrated on I, weakly crenulated on posterior half of II; absent on segments III–IV; ventrolateral carinae crenulated on I–III and serrated on IV; ventromedian carinae smooth on I, irregularly granulated on II, granulated on III, and crenulated on IV. Dorsolateral carinae of segment IV terminate at articulation condyle. Segment V: dorsolateral carinae serrated; lateral carinae irregularly crenulated for two-fifths of posterior aspect; ventrolateral and single ventromedian carinae serrated; ventromedian carina not bifurcated, terminating in straight line. Anal arch with 13 small serrated granules. Intercarinal areas of segments I–V essentially smooth. Segments I–V with numerous long setae on ventral, lateral and dorsal aspects.

TELSON (Fig. 205). Vesicle elongated, with highly curved aculeus. Vesicle essentially void of granules; distal half of ventral surface with scattered elongated

Figure 202: *Iurus kinzelbachi*, **sp. nov.**, dorsal and ventral views. Holotype male, Aydın Province, Dilek Peninsula National Park, Turkey.

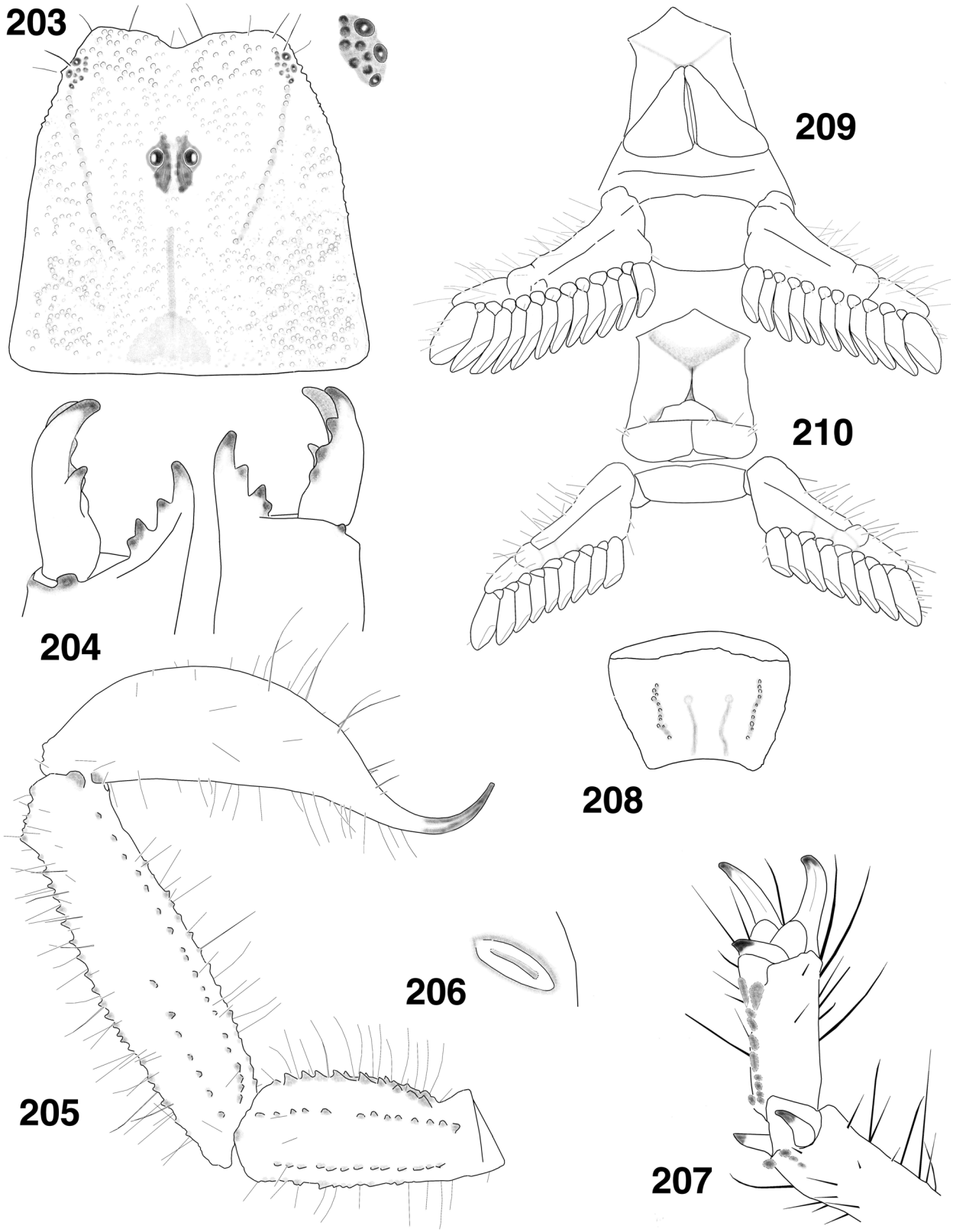

Figures 203–210: *Iurus kinzelbachi*, **sp. nov.,** Dilek Peninsula National Park, Aydın, Turkey. **203–209.** Male holotype. **210.** Female paratype. **203.** Carapace and close-up of lateral eyes. **204.** Right chelicera, ventral and dorsal views. **205.** Telson and metasomal segments IV–V, lateral view. **206.** Stigma. **207.** Tarsus and partial basitarsus, left leg IV. **208.** Sternite VII. **209.** Sternopectinal area. **210.** Sternopectinal area.

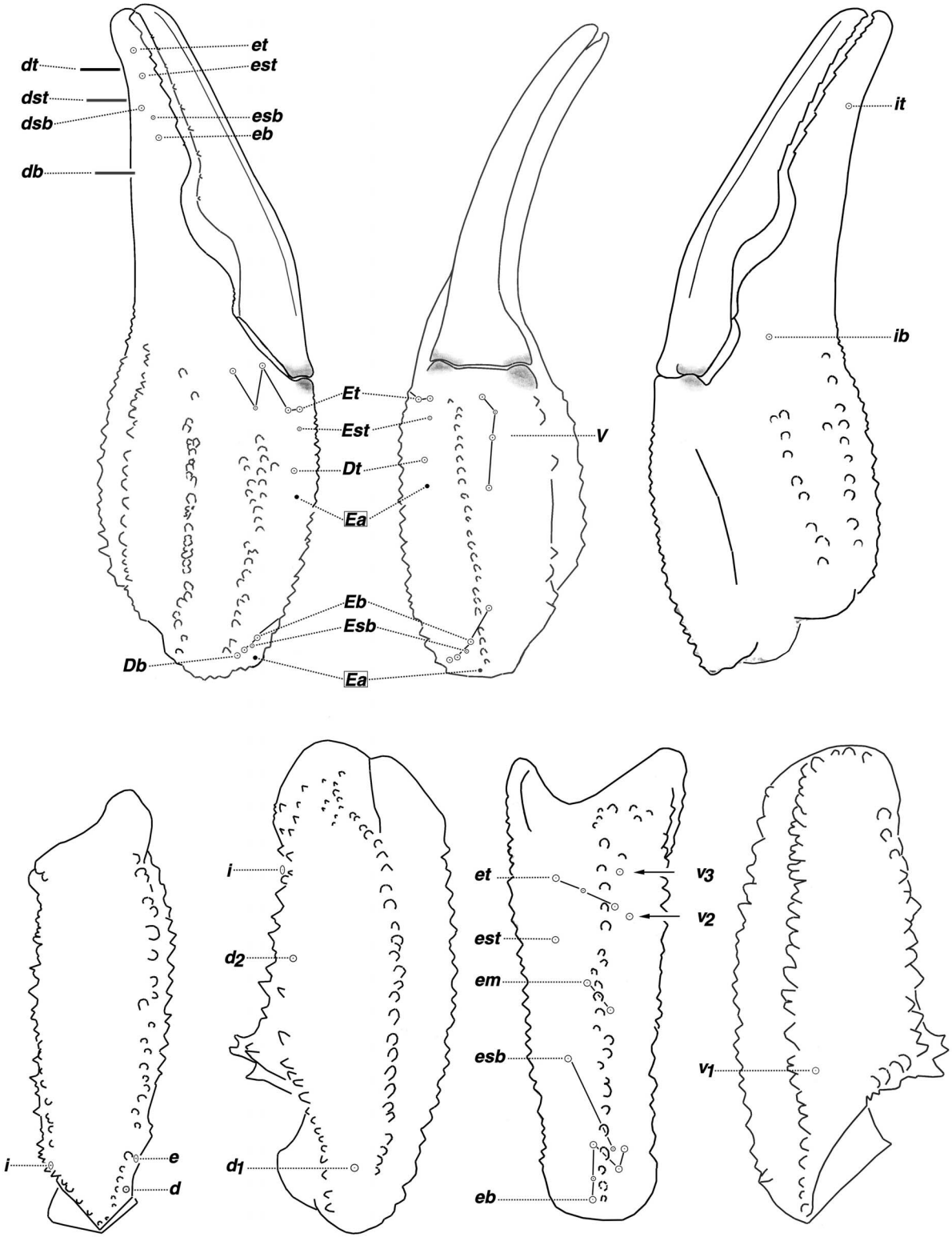

Figure 211: Trichobothrial pattern of *Iurus kinzelbachi* **sp. nov.**, male holotype. Dilek Peninsula National Park, Aydın, Turkey. Note presence of two external petite accessory trichobothria (*Ea* inside rectangle) on the chela representing types 8 and 9, exclusively found in *I. kinzelbachi*.

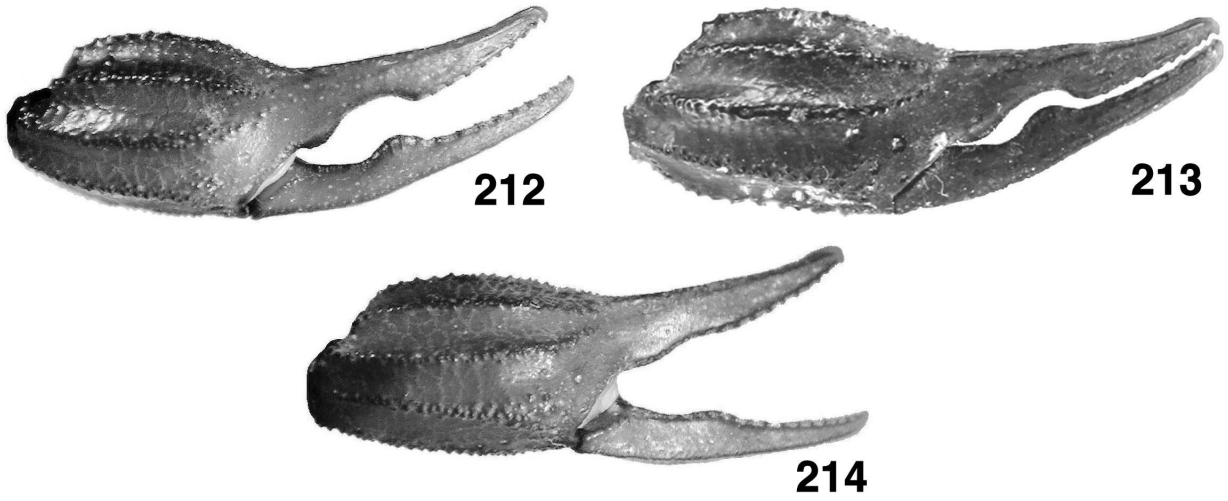

Figures 212–214: Chela, lateral view, *Iurus kinzelbachi* **sp. nov. 212.** Male, Naldöken ("Narli Kioi"), İzmir, Turkey. **213.** Male, Dilek Peninsula, Aydın, Turkey. **214.** Female, Naldöken ("Narli Kioi"), İzmir, Turkey. Note, in the adults the movable finger lobe is positioned proximal of finger midpoint, and a moderate fixed finger proximal gap exists in the males.

curved setae, basal half essentially void of setation; dorsal surface irregularly scattered with short to medium length setae; base of aculeus with setation ventrally and dorsally. Vesicular tabs with small rounded granules ventrally.

PECTINES (Fig. 209, paratype female Fig. 210). Well-developed segments exhibiting length|width formula 916|505. Sclerite construction complex, three anterior lamellae and one large middle lamella with slight indications of a smaller distal sclerite; fulcra of medium development. Teeth number 11/12. Sensory areas developed along most of tooth inner length on all teeth, including basal tooth. Scattered setae found on anterior lamellae and distal pectinal tooth. Basal piece large, with subtle swallow indentation along anterior edge, length|width formula 335|505.

GENITAL OPERCULUM (Fig. 209). Sclerites triangular, longer than wide, separated for entire length. Genital papillae visible between sclerites but do not extend beyond genital operculum posterior edge (see discussion on female below).

STERNUM (Fig. 209). Type 2, posterior emargination present, well-defined convex lateral lobes, apex visible but not conspicuous; anterior portion of genital operculum situated proximally between lateral lobes; sclerite longer than wide, length|width formula 290|260; sclerite slightly tapers anteriorly, posterior-width|anterior-width formula 485|415 (see discussion on female below).

CHELICERAE (Fig. 204). Movable finger dorsal edge with one large subdistal (*sd*) denticle; ventral edge with one large pigmented accessory denticle at finger midpoint; ventral edge serrula not visible. Ventral distal denticle (*vd*) slightly longer than dorsal (*dd*). Fixed finger with four denticles, median (*m*) and basal (*b*) denticles conjoined on common trunk; no ventral accessory denticles present.

PEDIPALPS (Fig. 211). Well-developed chelae, with long fingers, heavily carinated, conspicuous scalloping on chelal fingers: well-developed lobe on movable finger, positioned proximal of midpoint in ratio 0.47; proximal gap present on fixed finger. **Femur:** Dorsointernal, dorsoexternal and ventrointernal carinae serrated, ventroexternal irregularly serrated. Dorsal surface smooth, ventral surface with minute granules medially, internal and external surface with line of 11 and 14 serrated granules, respectively. **Patella:** Dorsointernal and ventrointernal carinae serrated, dorsoexternal crenulated and ventroexternal serrated, and exteromedian carina strong, serrated, and singular. Dorsal and ventral surfaces smooth; external surface with serrated exteromedian carina; internal surface smooth with well-developed, doubled DPS and VPS. **Chelal carinae:** Complies with the "8-carinae configuration". Digital (*D1*) carina strong, granulated; dorsosecondary (*D3*) and dorsomarginal (*D4*) rounded, heavily granulated; dorsointernal (*D5*) irregularly serrated; ventroexternal (*V1*) strong and serrated, terminating at external condyle of movable finger; ventrointernal (*V3*) rounded, smooth to granulated, continuous to internal condyle; external (*E*) heavily granulated, irregular distally; internal (*I*) irregularly serrated. **Chelal finger dentition:** Number of median rows, internal denticles (*ID*), and outer denticles (*OD*) are difficult to determine due to conspicuous scal-

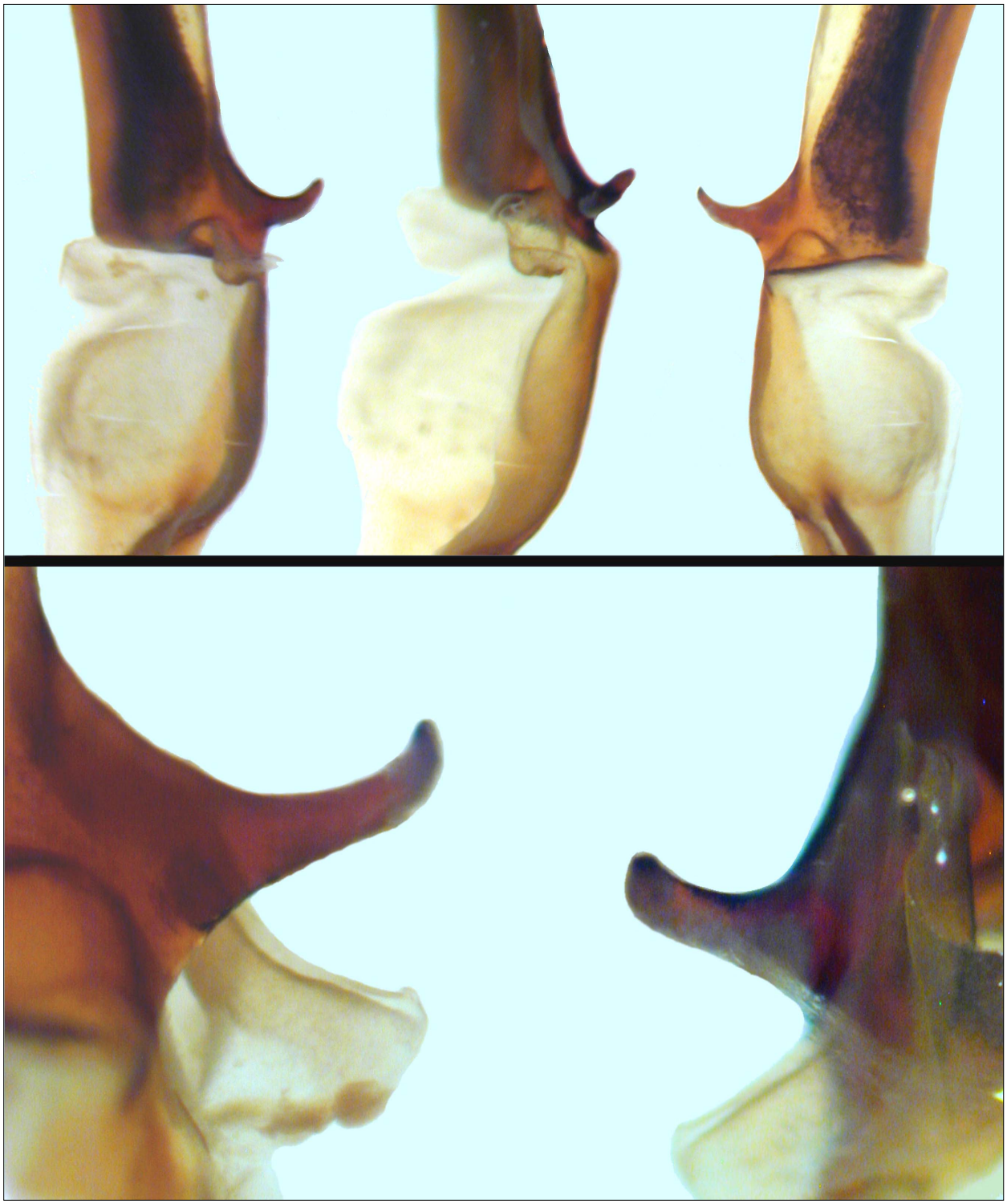

Figure 215: Close-up of median area of hemispermatophore, *Iurus kinzelbachi*, **sp. nov.**, paratype, Dilek Peninsula National Park, Aydın, Turkey. **Top.** Left hemispermatophore, ventral, ventrointernal, and dorsal views. **Bottom.** Right hemispermatophore, close-up of acuminate process showing the blunt terminus. The paraxial organ sleeve attachment to the seminal receptacle is visible in the ventral view of these photographs.

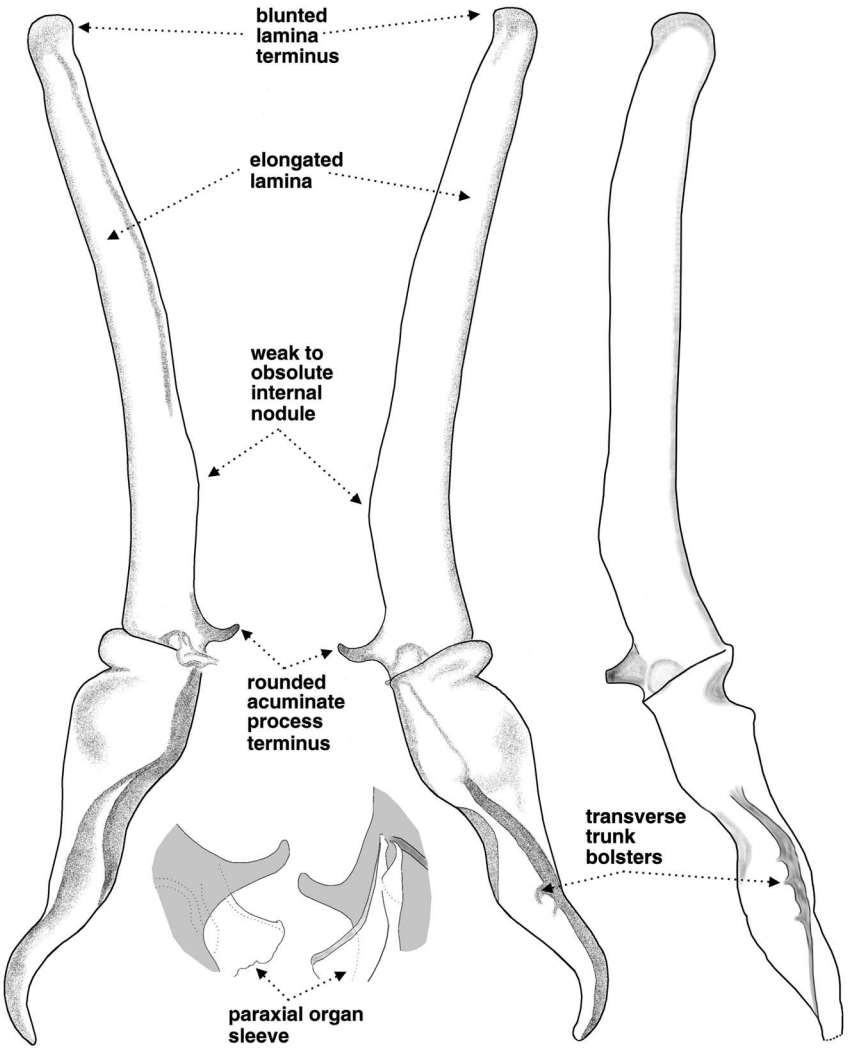

Figure 216: Hemispermatophore of *Iurus kinzelbachi*, **sp. nov.**, paratype**. Left & Center.** Ventral and dorsal views, Dilek Peninsula National Park, Aydın, Turkey. **Right.** Dorsal view, Naldöken ("Narli Kioi"), İzmir, Turkey, paratype; note that tip of acuminate process is missing. Diagnostic of this species is the elongated lamina with blunted terminus, shown in both hemispermatophores, a somewhat weak to obsolete internal nodule, transverse trunk bolsters, and a rounded acuminate process terminus. **Bottom.** Close-up of the attachment of the paraxial organ sleeve to the seminal receptacle (right hemispermatophore).

loping of the fingers. Median denticle (*MD*) row groups oblique and highly imbricated; 11/11 *ID*s to socket beginning on fixed finger and 14/14 *ID*s on movable finger; 14/14 *OD*s on fixed finger and 11/11 *OD*s to lobe center on movable finger. No accessory denticles present. **Trichobothrial patterns (Fig. 211):** Type C, neobothriotaxic, a single petite accessory trichobothrium in *Est* series (type-8), both chelae, and *Esb* series (type-9), right chela only.

LEGS (Fig. 207). Both pedal spurs present on all legs, lacking spinelets; tibial spurs absent. Tarsus with conspicuous spinule clusters in single row on ventral surface, terminating distally with a pair of enlarged spinule clusters. Unguicular spine well-developed and pointed.

HEMISPERMATOPHORE (Figs. 215–216). The hemispermatophore of the holotype has not been examined, therefore this description is based on two paratype specimens from İzmir and Dilek Peninsula. The hemispermatophore of *I. kinzelbachi* is unique among *Iurus* species, exhibiting the most elongated lamina, rounded terminus, weak to obsolete internal nodule, presence of transverse trunk bolsters, and a round acuminate process terminus (more data below).

Male and female variability. As seen in Figures 212–214, the adult female does not exhibit a proximal gap and the movable finger lobe is not as developed as in the male. There is no significant sexual dimorphism in morphometrics. Though the male has a thinner metasoma, the MVDs (L/W) only ranged from 7.1 to 9.2 %. Pectinal tooth counts in males exceed those of females by approximately 1.3 teeth, male 10–12 (10.62) [24], female 8–11 (9.33) [36] (see histograms in Fig. 73). The genital operculum of the male is dramatically different from that in the female (Figs. 209–210). The sclerites, subtriangular in shape, are as long as or longer than wide in the male, whereas in the female the sclerites

	***Iurus kinzelbachi* sp. nov.**		
	Dilek Peninsula, Adyın, Turkey	**Naldöken, İzmir, Turkey**	
	Male Holotype	**Male Paratype**	**Female Paratype**
Total length	78.35	75.05	80.55
Carapace length	10.40	10.80	12.30
Mesosoma length	25.35	20.55	22.85
Metasoma length	30.20	31.30	32.55
Segment I length/width	3.95/4.60	3.95/4.70	4.10/5.20
Segment II length/width	4.55/3.90	4.70/4.10	4.90/4.45
Segment III length/width	5.05/3.70	5.20/3.70	5.35/4.00
Segment IV length/width	6.10/3.35	6.35/3.30	6.50/3.60
Segment V length/width	10.55/3.00	11.10/3.15	11.70/3.25
Telson length	12.40	12.40***	12.85***
Vesicle length	8.20	8.65	9.40
width/depth	3.30/3.05	3.50/3.20	3.65/3.35
Aculeus length	4.20	3.75***	3.45***
Pedipalp length	44.15	44.55	49.25
Femur length/width	11.20/3.65	11.25/3.45	12.65/4.00
Patella length/width*	10.70/2.80	10.45/4.05	11.20/4.30
DPS height**	1.40	1.35	1.55
Chela length	22.25	22.85	25.40
Palm length	10.40	10.45	11.55
width/depth	5.70/7.50	6.00/7.65	6.30/8.00
Fixed finger length	11.10	12.00	13.25
Movable finger length	14.15	14.45	15.65
Pectines teeth	11-12	10-10	9-9
middle lamellae	3-2	3-3	1-1++
Sternum length/width	2.90/2.60	2.35/2.80	3.45/3.35

Table 10: Morphometrics (mm) of *Iurus kinzelbachi* **sp. nov.** * Patella width is widest distance between the dorsointernal and externomedial carinae. ** DPS height is from tip of spines to dorsointernal carina center.

are short and wide, more than twice as wide as long. Whereas the sclerites are fused medially in the female, they are separated along their entire length in the male, exposing significantly developed genital papillae. The enlarged genital operculum of the male extends distally between the lateral lobes of the sternum partially obscuring its proximal region. Figures 223–226 show dorsal and ventral views of both male and female specimens, the map of distribution for this species, and photographs of its type locality.

Discussion

Unique in this species is the combination of a proximal gap in the adult male and a proximally positioned movable finger lobe. All other *Iurus* species that exhibit a proximal gap also have a distally placed lobe in adults. The movable finger lobe ratio is larger in the male than the female, 0.44–0.47 vs. 0.40–0.42 (ratios calculated from adults with carapaces 10 mm or larger; see scatter chart in Fig. 56 for a complete analysis of this character).

I. kinzelbachi, statistically, has the overall smallest number of pectinal teeth (Fig. 73), but *I. dufoureius* is quite close, exhibiting only a small fractional difference; *I. kraepelini*, with the largest number of teeth, averages roughly two more pectinal teeth per gender than *I. kinzelbachi*.

The hemispermatophore of *I. kinzelbachi* has been examined from material representing both of its major reported localities (see map in Fig. 60), Aydın and İzmir provinces. The unique and unusual morphology of this hemispermatophore is consistent in the three examined for this study (Figs. 215–216). The lamina is quite elon-

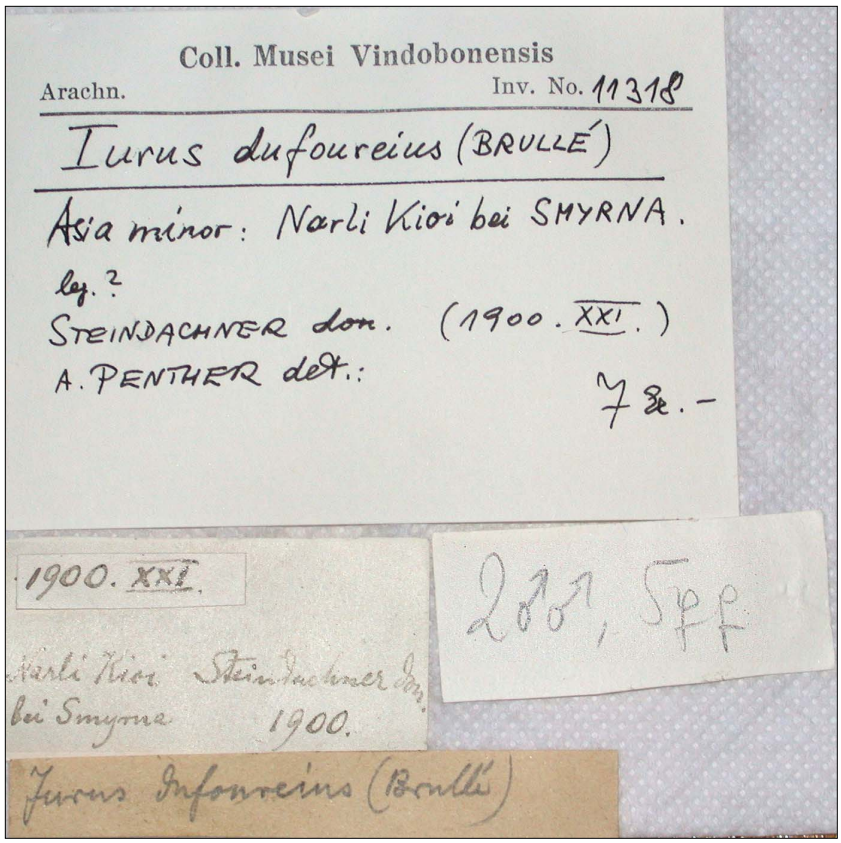

Figure 217: Set of labels for seven specimens of *Iurus kinzelbachi*, **sp. nov.**, from Narli Kioi (= Naldöken), İzmir, Turkey. Collected in 1900.

gated, at least 1.5 times longer than the trunk with the ratio 1.513–1.571 (1.546) [3] (see Table 2), the relatively longest lamina in the genus. The lamina terminus is somewhat blunted, not pointed, though this appearance is due, in part, to the somewhat subparallel and narrow lamina base edges. Also unique in this hemispermatophore is the rounded or near obsolete internal nodule. This vestigial nodule is situated quite basal on the lamina, in a ratio 4.313–5.107 (4.710) [2], exceeding other species hemispermatophores by at least 39 %. As depicted in Table 3, *I. kinzelbachi* exceeds the other species in all four morphometric ratios, all indicators of the elongated lamina found in this species. Finally, the acuminate process terminus is rounded not truncated as in the other *Iurus* species, and transverse trunk bolsters are present. The paraxial organ sleeve was present in two of the three hemispermatophores examined (Figs. 215–216); its attachment to the seminal receptacle is as found in other species.

In Appendix C we present a complete analysis of the morphometric trends across the five species of *Iurus*. From this analysis, we see that the chelal finger lengths in *I. kinzelbachi* dominated in a large majority of morphometric ratio comparisons: averaging 21 and 22 comparsions out of 25 for the male and 20 and 23 for the female. Of equal importance, this analysis also indicates morphometrics that dominated the *least* in ratio comparisons. In *I. kinzelbachi* the telson width dominated only 5–6 morphometrics out of 25 (i.e., *I. kinzelbachi* has a relatively thin telson vesicle). We constructed two ratios, the movable finger and fixed finger lengths divided by the telson width, comparing *I. kinzelbachi* to the other four species for both genders. These two ratios provide excellent diagnostic characters separating *I. kinzelbachi* from *I. dufoureius* and *I. kraepelini*, the species closest geographically to *I. kinzelbachi*: MVDs for *I. dufoureius* are 26.1–27.8 % and 22.8–28.5 % for fixed and movable fingers, respectively, and for *I. kraepelini* are 23.0–28.4 % and 12.9–19.3 for fixed and movable fingers, respectively (note, ranges represent both genders). These ratios also provide separation from *I. asiaticus* but the MVDs were considerably smaller, ranging 11.6–12.4 % and 6.4–8.8 % for fixed and movable fingers. The ratios were essentially equal when compared with *I. kadleci*, another species with a thin telson.

Soleglad, Kovařík & Fet (2009) reported for the first time neobothriotaxy in genus *Iurus*. Although nine types and 77 occurrences of neobothriotaxy were reported in their study, spanning 101 specimens, they occurred sparingly, many times only on a single pedipalp, and many trichobothria were petite in size. In

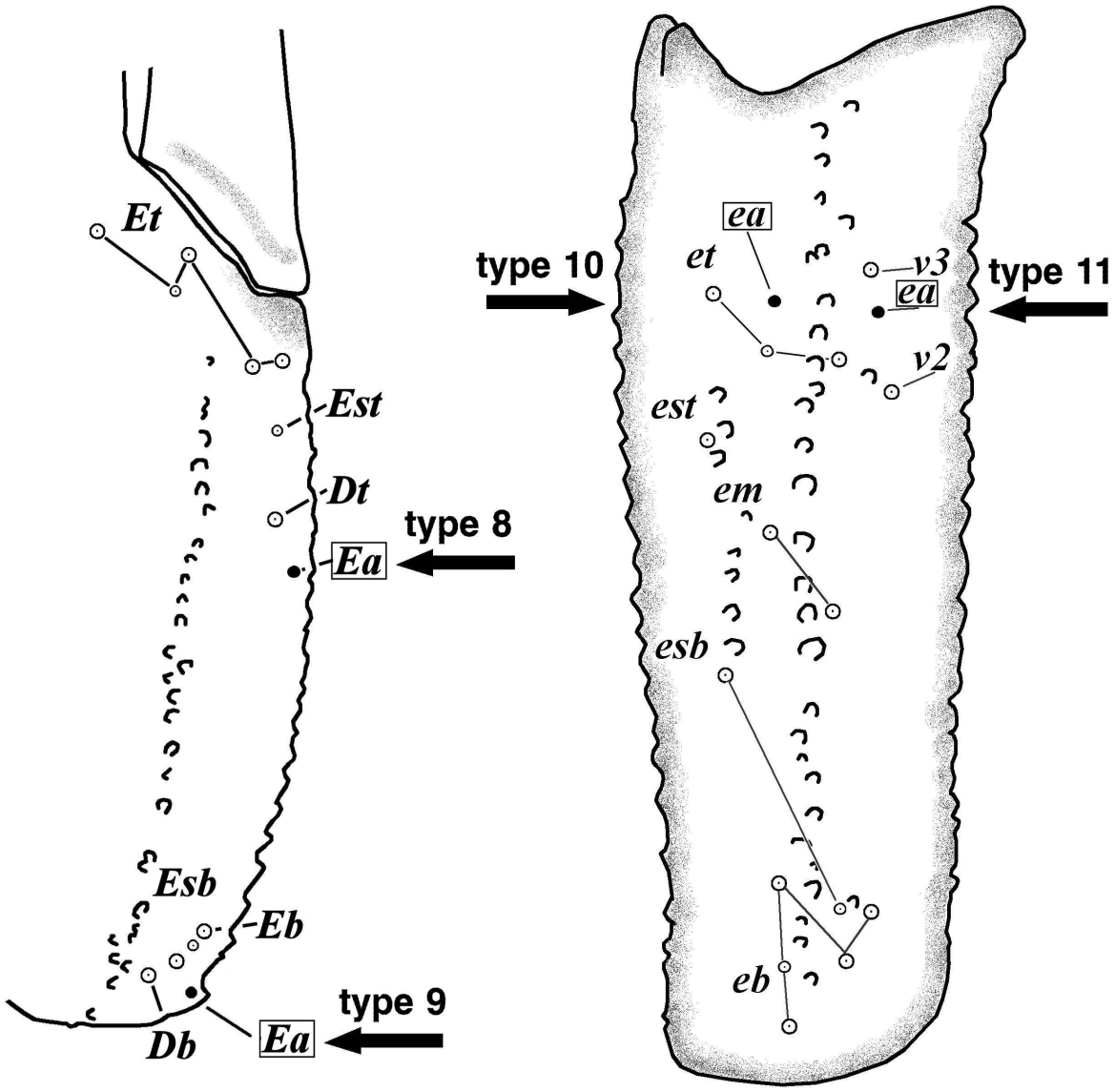

Figure 218: Partial trichobothrial pattern illustrating neobothriotaxy in *Iurus kinzelbachi*, **sp. nov**. **Left.** Chelal *Est* series, one accessory trichobothrium (*Ea*); *Eb* series, one accessory trichobothrium (*Ea*). **Right.** Patellar *et* series, two *types* of accessory trichobothria (*ea*). Note that all accessory trichobothria are *petite* in size and in some cases may be vestigial. Accessory trichobothria are represented by closed circles. See Appendix B for a complete synopsis of neobothriotaxy in *Iurus*.

this study, two types of neobothriotaxy were reported, unique in the genus, found in an isolated population of seven specimens from the western coast of Turkey, near İzmir. We have examined an additional series of 23 specimens from the Dilek Peninsula National Park, Aydın, Turkey, and discovered they also exhibited these two specific types of neobothriotaxy. We concluded from the analysis of neobothriotaxy alone that the two populations belonged to the same species that also is a new one, *I. kinzelbachi*. In addition, two more neobothriotaxic types were detected in the Dilek population, making a total of four types unique to *I. kinzelbachi*. Figure 218 illustrates the four types of neobothriotaxy diagnostic of *I. kinzelbachi*: two accessory trichobothria found on the chela, one each in the *Est* and *Esb* series, and two accessory trichobothria on the external aspect of patella, both in the *et* series. These accessory trichobothria are petite in size, some on the chela are reduced in size to be classified as "small petite" while others, at best, can be described only as vestigial. Figures 219–222 present close-up photographs of these four neobothriotaxic types representing both populations

Locality	Specimen	Chela Types 8 & 9 *Est* Series, *Eb* Series		Patella Type 11 *et* series		Patella Type 10 *et* series	
		left	right	left	right	left	right
İzmir, İzmir, Turkey	A ♂	vestigial*, -	petite*, -	-	-	-	-
	A ♀	sm. petite*, petite	petite*, -	petite*	-	-	-
	SA ♂	vestigial, -	vestigial, -	-	-	-	-
	J ♀	vestigial, -	vestigial, -	-	petite*	-	-
	SA ♀	vestigial, vestigial	petite*, -	-	-	-	-
	SA ♀	petite*, -	petite*, vestigial	-	petite*	-	-
	A ♀	vestigial*, -	vestigial, -	-	petite*	-	-
Dilek Peninsula, Aydın, Turkey	A ♂	-, -	-, -	-	-	petite*	-
	A ♀	-, -	-, -	-	petite*	-	-
	A ♂	petite*, -	petite, petite	-	-	-	-
	A ♀	vestigial, -	-, -	-	-	-	-
	A ♀	-, -	petite, -	-	-	-	-
	A ♀	-, -	-, -	-	-	-	-
	A ♀	-, -	-, -	-	-	-	-
	SA ♂	-, petite	petite, -	-	-	-	-
	SA ♂	-, -	-, vestigial	-	-	-	-
	A ♂	vestigial, -	-, vestigial	-	-	-	-
	SA ♂	vestigial, -	-, small petite*	-	-	-	-
	A ♀	-, -	-, petite	-	-	-	-
	A ♀	-, -	-, -	-	-	-	-
	A ♀	-, -	-, petite	-	-	-	-
	A ♀	-, petite	petite, petite	-	-	-	-
	SA ♂	-, -	-, -	-	-	-	-
	SA ♂	-, -	-, -	-	-	petite	-
	SA ♀	-, small petite	-, -	-	-	-	-
	SA ♂	vestigial, -	petite, sm. petite	-	-	-	-
	A ♂	-, -	-, -	-	-	-	-
	A ♀	-, -	-, -	-	-	-	-
	A ♀	-, -	-, small petite	-	-	-	-
	A ♀	-, -	-, -	petite	-	-	-
♂ petite: 7 (12) 58 % **♂ vestigial: 3 (12) 25 %** **♂ total: 10 (12) 83 %**		***Esb*:** **petite: 12 (60) 20 %** **vestigial: 12 (60) 20 %** **total: 24 (60) 40 %**		**total: 6 (60) 10 %**		**total: 2 (60) 3 %**	
♀ petite: 13 (18) 72 % **♀ vestigial: 1 (18) 6 %** **♀ total: 14 (18) 78 %**		***Eb*:** **petite: 11 (60) 18 %** **vestigial: 4 (60) 7 %** **total: 15 (60) 25 %**					
♂ & ♀: 24 (30) 80 %							

Table 11: Statistics on four types of neobothriotaxy found exclusively in *Iurus kinzelbachi*, **sp. nov**. These accessory trichobothria are classified as petite, small petite, and vestigial. This data shows that 80 % of the 30 specimens examined exhibited at least vestigial to petite accessory trichobothria, 70 % of which were petite. Neobothriotaxy in the *Esb* series was the most prevalent, occurring in 40 % of the specimens, whereas patellar type 10 was the rarest, only detected in 3 %. * indicates neobothriotaxy illustrated in Figures 219–222. See Appendix B for overview of all neobothriotaxic types across all species of *Iurus*.

of *I. kinzelbachi*, both left and right pedipalps, and full and small petite, as well as vestigial types. Table 11 presents a complete analysis of the occurrence of neobothriotaxy in all 30 specimens of *I. kinzelbachi* examined. We see that 80 % of the specimens exhibited at least one accessory trichobothrium; only six specimens, all from Aydın, lacked accessory trichobothria. All specimens from İzmir had at least one accessory trichobothrium on each pedipalp, though in three specimens only vestigial. Six specimens from Aydın showed neobothriotaxy on both pedipalps. Neobothriotaxy on the chela was the most prevalent, being found

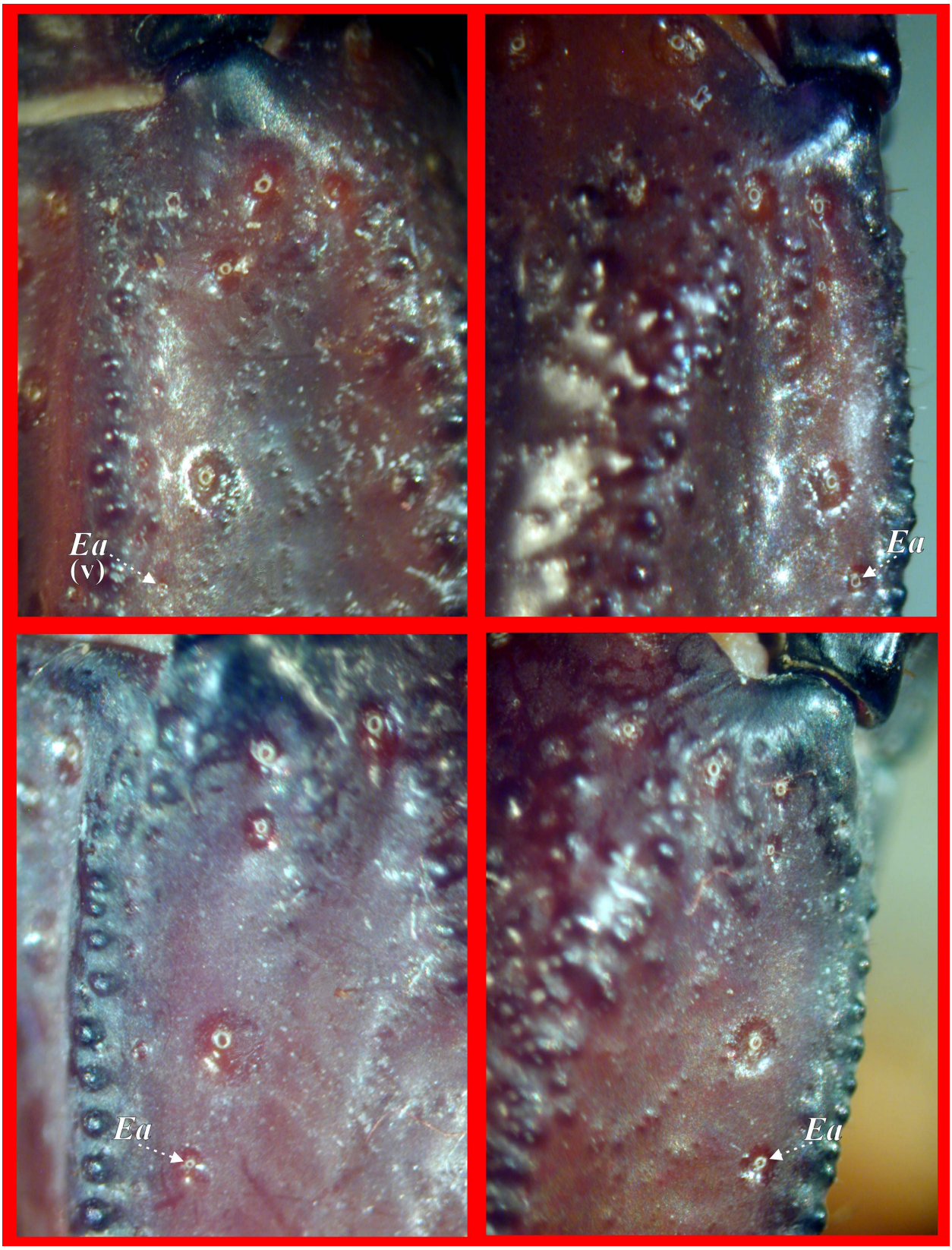

Figure 219: Neobothriotaxy on chela in *Iurus kinzelbachi*, **sp. nov**., Naldöken, İzmir, Turkey, type 8. **Top-Left.** Adult male, left chela, showing vestigial (v) *Ea*. **Top-Right.** Adult male, right chela. **Bottom-Left.** Adult female, left chela, showing small petite *Ea*. **Bottom-Right.** Adult female, right patella. Solitary accessory trichobothrium (*Ea*, marked in white) located in *Est* series.

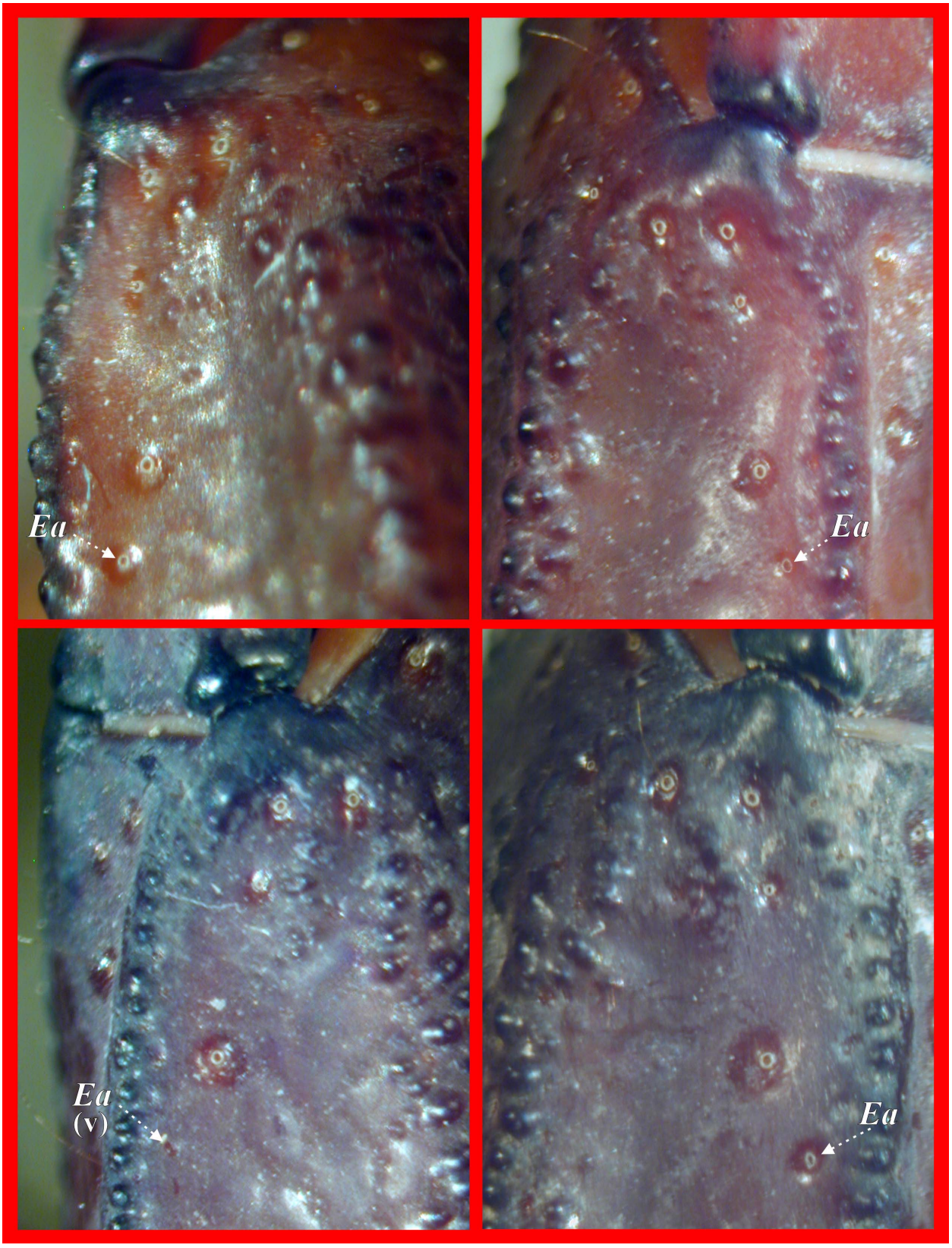

Figure 220: Neobothriotaxy on chela in *Iurus kinzelbachi*, **sp. nov**., Naldöken, İzmir, Turkey, type 8. **Top-Left.** Subadult female, left chela. **Top-Right.** Subadult female, right chela. **Bottom-Left.** Adult female, right chela, showing vestigial (v) *Ea*. **Bottom-Right.** Subadult female, right chela. Solitary accessory trichobothrium (*Ea*, marked in white) located in *Est* series.

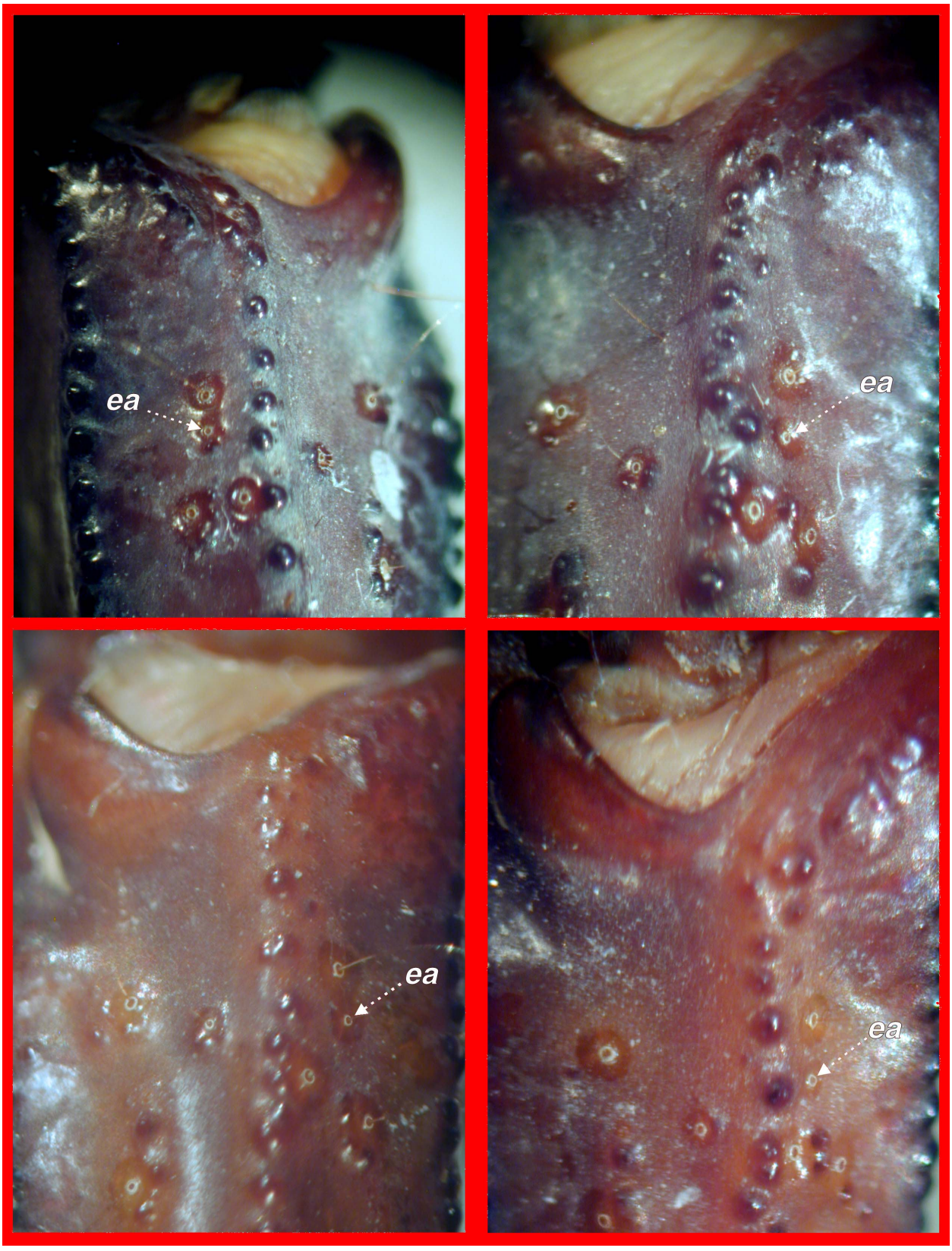

Figure 221: Neobothriotaxy on patella in *Iurus kinzelbachi*, **sp. nov.**, Naldöken, İzmir, Turkey, type 11. **Top-Left.** Adult female, left patella. **Top-Right.** Adult female, right patella. **Bottom-Left.** Juvenile female, right patella. **Bottom-Right.** Subadult female, right patella. Solitary accessory trichobothrium (*ea*, marked in white) is located in *et* series.

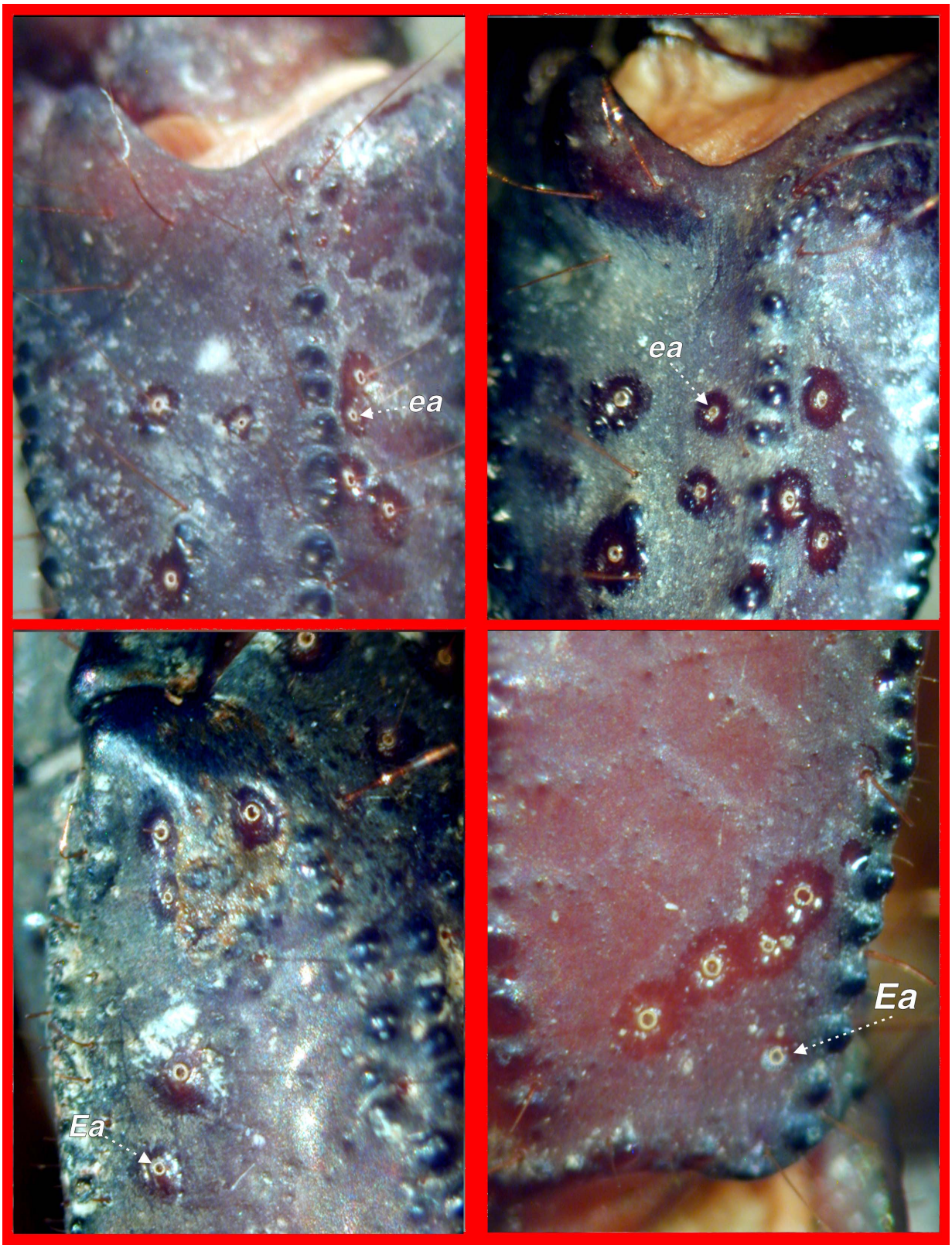

Figure 222: Neobothriotaxy on patella and chela in *Iurus kinzelbachi*, **sp. nov.**, Dilek Peninsula, Aydın, Turkey, types 8, 9, 10, 11. **Top-Left.** Adult female, right patella, type 11. **Top-Right.** Adult male, right patella, type 10. **Bottom-Left.** Adult male, left chela, type 8. **Bottom-Right.** Subadult male, right chela, type 9. Solitary accessory trichobothria (*ea* and *Ea*, marked in white) are located in *et* and, *Est* and *Eb* series, respectively.

Figure 223: *Iurus kinzelbachi*, **sp. nov.**, dorsal and ventral views. Paratype female, Aydın Province, Dilek Peninsula National Park, Turkey.

on 67 % of the specimens; neobothriotaxy on the patella was present only in 13 %. Although we consider this unique neobothriotaxy diagnostic of *I. kinzelbachi* and important in serious discussions of the overall evolution of the genus, we did not include it in the key since it is not found in all specimens or both chela.

Material Examined (= type material, 30 specimens). Holotype: ♂ (NHMW), TURKEY, *Aydın Province*: Söke District, Dilek Peninsula National Park, Canyon, 37°41'37"N, 27°09'37"E, 82 m asl, 18 June 2005, leg. H. Koç. **Paratypes: Turkey,** same label as holotype, 1 sbad. ♂, 1 ♀ (FKCP), 5 sbad. ♂, 9 ♀, 1 sbad. ♀, leg. H.

Figure 224: *Iurus kinzelbachi*, **sp. nov.**, dorsal view. Adult male, Aydın Province, Dilek Peninsula National Park, Turkey.